Liver Perfusion using Level Set Methods

Sebastian Nowozin, Lixu Gu

Digital Medical Image Processing and Image Guided Surgery Laboratory,
Shanghai Jiaotong University

Abstract. The family of Level Set Methods has been successfully used by scientists and practitioners for medical image processing. Image segmentation using active implicit contours is applied in 2D and 3D medical imaging, with the most popular methods being the Fast Marching Method and the Narrow band Level Set Method.

In this paper we apply level set segmentation to aid in automating the clinical challenge of measuring the contrast agent concentration in liver perfusion time series. For this, we apply implicit contour methods to time series of two-dimensional MRI images to yield accurate measurements of local image properties located relative to the shape of the liver across all images in the series.

Our results show that Level Set Methods can be used to provide the necessary segmentation shape data to reliably measure local image intensities positioned relative to this shape throughout a time series, where the location and shape of the object to be tracked changes.

1 Introduction

For certain illnesses related to the liver the blood flow to the liver has to be studied. By injecting a contrast agent into the patients body while taking MRI images in fixed time intervals, the concentration of the contrast agent can be studied while it flows through the patients body. A short time after the injection the contrast agent reaches the liver and the MRI images at that time can reveal important information about the blood supply condition of the liver for that patient. This information can lead to a more accurate diagnosis. The overall procedure is called *liver perfusion*.

Part of automating the above process can be modeled as a two dimensional registration problem, where the liver is the object of interest that is registered between the images. The more important problem is what to use as input to the registration mechanism. We use the segmented liver shape and now describe previous work on segmentation algorithms for two dimensional MRI images.

G. Hommel and Sheng Huanye (eds.), Human Interaction with Machines, 177-188.

An excellent discussion of medical image segmentation algorithms including level set methods is Suri et al. (Suri *et al.*, 2001a) and (Suri *et al.*, 2001b). The introduction of level set techniques into the field of medical image segmentation is due to Malladi in 1995 (Malladi & Sethian, 1995). Malladi used the curvature and the gradient of the image convolved with a Gaussian as a potential field to guide the evolution of the level set function. Our segmentation approach is based on his work, using a refined speed function. We have not found literature concerning the automation of perfusion measurements by incorporating level set methods for segmentation.

A large part of the effort to improve level set segmentation has been focused on merging a-priory knowledge or regional statistics into the speed function. This is necessary as a simple non-regional speed function will let the level set isocontour leak over weak or partially non-existing boundaries. Ho et al. (Ho *et al.*, 2001) replace the propagation term with a force based on regional statistics and let adjacent regions compete for a common boundary. They demonstrate improved results for brain tumor segmentation in MRI. Suri used fuzzy classifications of regions in (Suri, 2000) to build a speed function incorporating shape, region, edge and curvature information and applied the resulting model successfully to brain segmentation.

The current method to perform liver perfusion measurements is manual, because the patient breathes throughout the series and the liver moves vertically in a coronal view. As such the position of the blood vessel to be studied has to be marked in every single image. Then the intensity of the MRI image at these positions is plotted over time and from this the concentration curve of the contrast agent is deduced. The curve is used for further diagnosis.

In this paper we describe an automated method to locate the perfusion area within the time series of two-dimensional MRI images and present first results of the method applied to perfusion series. We have not found prior methods in the literature specific to liver perfusion measurements. Our method is novel in that it (a) combines segmentation results with a simple and efficient registration scheme specific to liver perfusion, (b) requires no manual interaction after a manual initialization and (c) can deal with small errors in the segmentated shape.

2 Methods

Now we describe briefly the fundamental methods we use througout the segmentation process.

2.1 Fast Marching Method

The Fast Marching Method (FMM) is an algorithm to efficiently solve curve and surface evolution problems. Consider a closed curve that evolves under a fixed-sign normal speed $F(x, y)$ dependent only on the position (x, y) in the computational domain. The curve either expands outward all the time or moves inward all the time and once a point has been crossed by the curve it will never be crossed again. Then, the Eikonal equation can be given as

$$|\nabla T|F = 1$$

where $T(x, y)$ is the arrival time at which the curve or surface crosses the given point (x, y). The Eikonal equation states the relationship that the gradient of arrival time is inversely proportional to the speed of the surface (Malladi & Sethian, 1996). The Fast Marching Method explicitly constructs the solution $T(x, y)$ for all points (x, y) in the domain. The complexity for N points is $O(N \log N)$ and the algorithm generalizes naturally to three or more dimensions. The original paper about the Fast Marching Method is from Sethian and Adalsteinsson (Adalsteinsson & Sethian, 1995). Since then, the Fast Marching Method has been intensively studied, the most detailed study is given by Sethian himself in (Sethian, 1998).

2.2 Narrow band Level Set Method

The level set method deals with the representation and evolution of closed interfaces, such as curves and surfaces. In the level set framework, the interface is *embedded* into a function of a dimensionality one higher than the original interface. Most often the signed distance function is used as embedding function, where the zero crossings of the function values represent the original interface. This implicit representation has many advantages. For one, geometric properties such as the local curvature κ and the normal

vector $\vec{N}$ can be easily determined. Most importantly, the evolution of the curve under the initial value problem

$$\phi_t + F\left|\nabla\phi\right| = 0$$

where ϕ is the embedding function, ϕ_t its derivate over time and F is the speed function, can be solved iteratively. The speed function F can be dependent on time dependent properties of the interface, such as the local curvature, the enclosed area and other global shape properties.

The level set method was first introduced in (Osher & Sethian, 1988), but since then the flexibility of the level set framework and the availability of high order accurate discretization methods have lead to adoption of the level set method in a large number of scientific fields, such as into computational physics, computer vision, image processing and medical image segmentation (Sethian, 1998), (Osher & Fedkiw, 2003).

The full level set method (Osher & Sethian, 1988) represents the curve on a discretized computational domain by assigning each point (i, j) in the domain a corresponding function value $\phi_{i,j}$. If one is interested only in the evolution and representation of the curve itself as opposed to the entire computational domain, it is enough to define ϕ within only a small boundary around the ZLC. This reduces the computational complexity significantly and is known as the Narrow band Level Set Method.

3 Segmentation

We developed a segmentation process for liver shape segmentation employing three steps. The first step locates a seed point for the segmentation in every image. The second step applies the Fast Marching Method to the original image at the given seed point to yield a first approximation of the liver shape. In the third step, this shape is used to initialize a level set segmentation step, which introduces a curvature reducing term to improve the segmentation results and repair local irregularities in the segmented shape. We now describe the steps in detail.

3.1 Locating the seed point

The seed point marks the initial curve position in the image. The initial curve is then evolved to segment the shape of the liver. The location of the

segmentation seed point is semi-automatic. For one image, the radiologist manually marks the segmentation seed point. For all other images it is located using the following robust, but specific method.

In the MRI perfusion series, there are two patterns, (a) the top of the liver shape is well contrasted to the background, and (b) as the patient breathes throughout the series, the liver moves only vertically. Combining these patterns, we construct a simple method to locate the seed point: for every image a gradient magnitude is extracted and slightly mean smoothed inside a vertical strip at the horizontal position of the initial seed point. The maximum gradient magnitude is located in the strip, and a fixed Δy is added to its vertical position. The value of Δy is determined once in the original image, for which we already know the seed point location.

3.2 FMM Segmentation Step

The FMM segmentation step takes as input all the images and a single seed point for each image. As result, a segmented liver shape is returned as bitmap of the same dimension as the input image. For each pixel in the map which has a positive truth value the pixel is thought to belong to the liver shape. The FMM algorithm is fairly straightforward and the only flexible part is the definition of the speed function to use and the stopping criteria. The speed function determines the propagation speed in normal direction for any point in the computational domain. The stopping criteria tells us when to stop the segmentation.

The speed function F_{FMM} we use for the FMM segmentation step is a thresholded variation of the well known speed function used in (Malladi & Sethian, 1995). We first define

$$F_{base}(x,y) = \frac{1.0}{1.0 + \left| S_k \cdot \nabla\left(G_\sigma * I_{x,y}\right)\right|^{S_p}}$$

which is the interface propagation speed in normal direction based on the gradient magnitude image. The gradient image $\nabla\left(G_\sigma * I_{x,y}\right)$ is the Sobel approximated gradient of the original image I convolved with a Gaussian of width σ. σ, S_k and S_p are constants and we had good results using $\sigma = 3.0$, $S_k = 13.0$ and $S_p = 2.0$ for the series examined. The speed image is generated from F_{base} by using it in the thresholded speed function F_{FMM}, which is defined

$$F_{FMM}(x,y) = \begin{cases} F_{base}(x,y) & F_{base}(x,y) \geq S_t \\ 0 & F_{base}(x,y) < S_t \end{cases}$$

with S_t being the threshold value. We used a quite high value of $S_t = 0.6$, because the FMM cannot incorporate curvature dependent information. A segmentation using an unthresholded speed function could leak out of the liver shape where the gradient is locally weak. By using a cautious threshold we limit the risk of leaking in exchange for a higher probability to not cover the entire liver shape in the first segmentation step. By using the more powerful and robust levelset evolution method in the next step, we overcome this defect. The stopping criteria for the FMM segmentation is simply a constant of the area size, which corresponds to the number of iterations of the FMM. The value is configurable but we choose a default of 1500 elements, which yielded good results.

3.3 Levelset evolution step

The input to the levelset evolution step is the first rough FMM segmentation result. In this step we incorporate a regularizing curvature term to smooth the shape, remove holes and refine the segmentation result. The result is the level set signed distance map for the entire computational domain.

We use a narrow band extending 6 elements into both directions. The speed function used is the original function used above plus a curvature regularizing term. It is

$$F(x,y,t) = \alpha \cdot -\kappa_{x,y,t} + F_{base}(x,y)$$

with $\alpha = 0.4$ constant, $\kappa_{x,y,t}$ being the local curvature at the point (x,y) at time t. The negative curvature term removes any small local irregularities the FMM segmentation has left over, such as sharp corners and single non-shape points within the shape due to noise in the original image. Globally it leads a smoother overall shape. We use a fixed number of evolution time steps of $\Delta t = 0.2$. To improve the results of the FMM segmentation, we found 80 time steps a good value. Finally, to simplify the perfusion area localization, the narrow band levelset function is extended to a full levelset in the entire domain by redistancing from the shape contour in the narrow band.

4 Perfusion Area Localization

We now introduce a new method to locate the perfusion area in each image given the segmented liver shape. In this method, the radiologist first marks the perfusion area in one image. Afterwards, this area is automatically located in all remaining images.

Our method is based on the following five observations. First, the movement of the liver is constrained to mainly vertical movements with only small horizontal movement. Second, shape of the segmented liver changes only slightly throughout the series. Third, rotation relative to the body is minimal and can be ignored. Fourth, the segmentation quality is not equal across the entire shape but the best at the top half of the liver, due to a strong gradient response there, while the weak gradient response in the lower half of the liver leads to more variation throughout the series. Fifth, when the contrast agent reaches the perfusion area a strong gradient response appears, which changes the segmentation result locally, up to the case of where the perfusion area is not considered part of the liver shape anymore. We now describe the details of the method. The idea is to anchor a coordinate system at each segmented shape which can be used to estimate a point location within and nearby the liver shape across all the images.

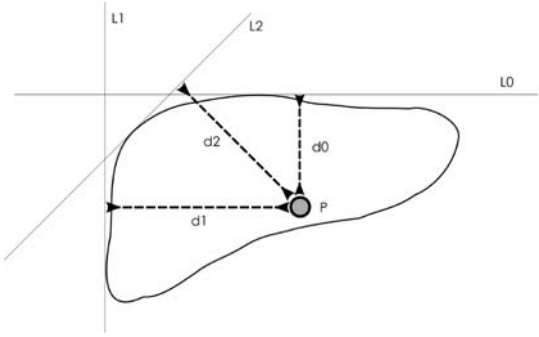

Fig. 1. A point P defined by a three element distance vector (d_0, d_1, d_2) relative to the lines L_0, L_1 and L_2.

Consider the point P in figure 1. Assume for now, we know for sure the absolute position of P in the image and that we have a good segmentation result of the liver shape. Then, we define a set of non-parallel lines $L = \{L_0, L_1, \ldots, L_n\}$. For each line L_k we determine the following for the

image I : 1. the distance $d(P_{x,y}, L_k, I)$ of every point $P_{x,y}$ within the segmented liver shape to L_k and 2. the shortest distance $d_s(L_k, I)$ among all $d(P_{x,y}, L_k, I)$. Then, any point within the liver in an image I can be represented as a *line relative distance vector* $D_{P_{x,y}}(I)$:

$$D_{P_{x,y}}(I) := \left(d(P_{x,y}, L_0, I) - d_s(L_0, I), \ldots d(P_{x,y}, L_n, I) - d_s(L_n, I)\right)$$

Using the above model, what remains to be discussed is how to find suitable lines to build the distance vector from and how to transfer from a given distance vector and the lines back to an absolute coordinate. The first question can be answered by considering the fourth observation made above. We use lines which always have their minimum distance point at the boundary of the shape where the segmentation result is of good quality. For example by using a horizontal line above the liver as distance measurement line, the resulting component in the distance vector will accurately reflect the relative position to the top of the liver across all the images because there is a strong gradient response at the top of the liver. Similarly, the top left part of the liver is always well segmented and by fitting a diagonal line with a 45 degree angle, we yield another good element for the distance vector.

To obtain an absolute coordinate given $D_P(I_p)$ for the initial radiologist-marked image I_p and the segmentation results for all other slices, we determine the position within or nearby the segmented shape that minimizes an error term. Consider a two dimensional coordinate system, where two non-parallel lines are enough to define a base and any additional lines are redundant. This redundancy can be used to define an error term ε which describes how much the distance vector for a point (x_0, y_0) in image I_0 diverges geometrically from the distance vector of the original known perfusion area point (x_p, y_p) in the radiologist-marked image I_p:

$$\varepsilon(x_0, y_0, I_0) := \left| D_{P_{x0,y0}}(I_0) - D_{P_{xp,yp}}(I_p) \right|$$

The *error minimizing point* (x, y) in the image I is one of the points that minimizes $\varepsilon(x, y, I)$. To find this point we test all points (x, y) for which the level set value is below some small positive threshold value t and keep the minimal error point. Because the embedding function used with the levelset method is the signed distance function, a small positive value

t allows for points nearby the segmented shape to be found, which is necessary because of the fifth observation made above.

After all the minimizing error points are located in the images, the perfusion area is simply a circle area centered around the point in each image. Because the liver shape is deformed only slightly throughout the series and the circle area is invariant to rotation, it is a simple but sufficient approximation. For each image, the resulting perfusion intensity is the mean value of all the MRI intensity values within the circle area[1].

5 Experimental Results

In this section we evaluate our implementation of the proposed method. We created a new implementation of the Narrow band levelset method and the FMM, written in C. A prototype GUI was written in C# using the Gtk# toolkit. We evaluate the performance of the proposed method on three perfusion series. The series consists of two-dimensional 256x256 MRI images taken with a GE Medical Systems Genesis Signa system at the Shanghai First People Hospital. They show the patients abdomen in coronal view. The imaging parameters are the following: slice thickness 15.0, repetition time 4.7, echo time 1.2, magnetic field strength 15000, flip angle 60 degrees. The images were converted to the PNG file format using medcon[2] with the following options: `medcon -e 1 0 -fb-dicom -c png -f *.dcm`. The first series consists of 240 images, the second series of 59 images and the third series of 200 images.

The evaluation has been performed using our prototype GUI. In the GUI, one particular good image of the series is selected and the seed point and the perfusion area is manually marked. Afterwards the segmentation and perfusion measurement process is started, which produces the intensity curve with its minimal error term values.

[1] The unit of this intensity is arbitrary and to obtain the contrast agent concentration from it requires more effort and also depends on which agent is used.

[2] Medcon, medical image conversion tool, http://xmedcon.sourceforge.net/

Fig. 2. A processed example image from the first series. For this case, the marked perfusion area is outside the segmented liver shape, as explained in the text.

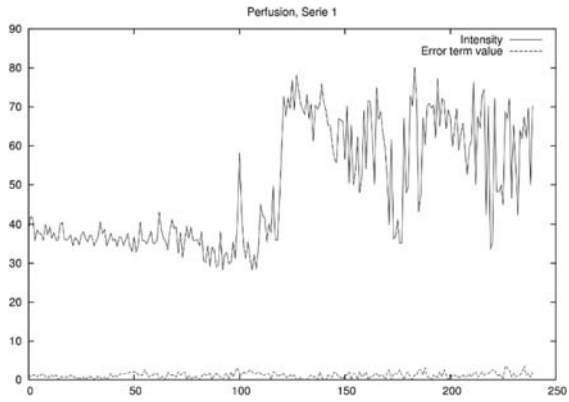

Fig. 3. The perfusion area intensity time curve and the corresponding error term values of the first perfusion series (240 images).

In figure 2 a typical processed image is shown. The seed point and the perfusion area is marked, and the segmented liver shape is drawn as overlay over the original image. The output intensity curve for the first series is shown in figure 3. Around the 120^{th} image, when the contrast agent reaches the liver, a strong response can be seen clearly. The error term values are also shown. They do not reflect the absolute accuracy of the located liver perfusion area. Instead they allow to give a relative comparison between the individual images.

Table 1. Error term comparison for the three example perfusion series.

Series	Images	Error mean	Error maximum	Error standard deviation
Series 1	240	1.1401	3.5355	0.7348
Series 2	59	2.9098	5.5227	1.5197
Series 3	200	2.5054	7.0356	1.6348

In table 1 we analyze the error terms within the three series. Interpreting the error values as the geometric distance from an optimal fit, the low mean error values for all the series indicates a good perfusion area localization success, which is confirmed by manually inspecting the processed images. For the runtime performance evaluation, the first series has been used. The system is a Pentium-M 1500Mhz, 512Mb RAM system.

Table 2. Runtime performance measurements.

Step	time	time per image
Locating seed point	44s	0.183s
FMM and levelset liver segmentation	443s	1.845s
Locating perfusion area	23s	0.095s
Total	510s	2.125s

6 Discussion and Conclusions

We proposed and evaluated a combined segmentation and registration method to extract local image intensity from the liver. For this we developed a simple and robust registration method which maps the perfusion area to a minimum error fit coordinate in each image.

The results still have to be verified for its clinical value by radiologists. We confirmed that the combined FMM and Narrow band Level Set Methods based segmentation approach is computationally efficient.

In the near future we will seek for confirmation and advice from radiologists to improve on this results. Also, further research is needed to draw conclusions about the performance of the proposed method in case the segmented objects have a more complex shape or vary considerably across the images in the series, such as the heart. In our method the quality of the measurement increases with improved segmentation results and we consider incorporating a model-driven segmentation approach to improve accuracy.

References

1. Adalsteinsson, D., & Sethian, J. 1995. A Fast Level Set Method for Propagating Interfaces.
2. Ho, Sean, Bullitt, Elizabeth, & Gerig, Guido. 2001 (11). Level Set Evolution with Region Competition: Automatic 3-D Segmentation of Brain Tumors. Tech. rept. TR01-036.
3. Malladi, R., & Sethian, J. A. 1995. Image Processing via Level Set Curvature Flow. *Proc. Natl. Acad. of Sci.*, **92**(15), 7046-7050.
4. Malladi, R., & Sethian, J. A. 1996. An O(N log N) algorithm for shape modeling. *Proceedings of the National Academy of Sciences*, **93**(Sept. 25), 9389-9392.
5. Osher, Stanley, & Fedkiw, Ronald. 2003. *Level Set Methods and Dynamic Implicit Surfaces*. Springer.
6. Osher, Stanley, & Sethian, James A. 1988. Fronts Propagating with Curvature-Dependent Speed: Algorithms Based on Hamilton-Jacobi Formulations. *Journal of Computational Physics*, **79**, 12-49.
7. Sethian, J. 1998. Level Set Methods and Fast Marching Methods: Evolving Interfaces in Computational Geometry. Cambridge University Press.
8. Suri, J., Liu, K., Singh, S., Laxminarayana, S., & Reden, L. 2001a. Shape Recovery Algorithms Using Level Sets in 2-D/3-D Medical Imagery: A State-of-the-Art Review.
9. Suri, J.S. 2000. Leaking prevention in fast level sets using fuzzy models: an application in MR brain. *IEEE EMBS International Conference on Information Technology Applications in Biomedicine, 2000. Proceedings*, 220-225.
10. Suri, J.S., Setarehdan, S.K., & Singh, S. 2001b. Advanced Algorithmic Approaches to Medical Image Segmentation: State-of-the-Art Applications in Cardiology, Neurology, Mammography and Pathology. Springer.